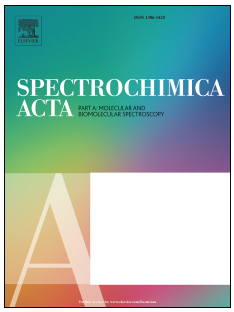

Entrapment in micellar assemblies switches the excimer population of potential therapeutic luminophore azapodophyllotoxin

Soham Mukherjee, Smruti Gupta, Kapil Ganorkar, Ajay Kumar, Sujit Kumar Ghosh

PII: S1386-1425(19)31113-8

DOI: https://doi.org/10.1016/j.saa.2019.117723

Reference: SAA 117723

To appear in: *Spectrochimica Acta Part A: Molecular and Biomolecular Spectroscopy*

Received Date: 15 June 2019

Revised Date: 19 September 2019

Accepted Date: 27 October 2019

Please cite this article as: S. Mukherjee, S. Gupta, K. Ganorkar, A. Kumar, S.K. Ghosh, Entrapment in micellar assemblies switches the excimer population of potential therapeutic luminophore azapodophyllotoxin, *Spectrochimica Acta Part A: Molecular and Biomolecular Spectroscopy* (2019), doi: https://doi.org/10.1016/j.saa.2019.117723.

Table of Contents Entry

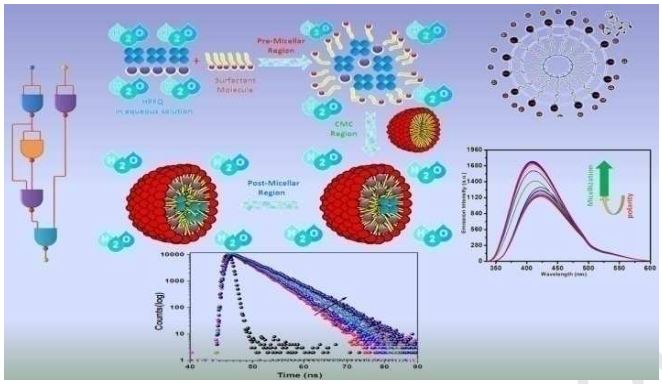

TOC represents localization therapeutic Azapodophyllotoxin in differently charged micellar assemblies which enhances the imaging capability by virtue of switching its excimer population.

Entrapment in micellar assemblies switches the excimer population of potential therapeutic luminophore Azapodophyllotoxin

Soham Mukherjee[$,&], Smruti Gupta[$], Kapil Ganorkar[$], Ajay Kumar[#] and Sujit Kumar Ghosh*[,$]

[$]*Department of Chemistry, Visvesvaraya National Institute of Technology, Nagpur, Maharashtra 440010, India*

[#] *School of Science, Technology and Environment, Universidad Ana G. Mendez-Cupey Campus, San Juan, PR, USA 00926*

[&]The present address of this author is as follows:

Department of Chemistry and Chemical Biology, Cornell University, Ithaca, New York 14850, USA

Corresponding Author

Dr. Sujit Kumar Ghosh, Department of Chemistry, Visvesvaraya National Institute of Technology, Nagpur, Maharashtra 440010, India, e-mail: sujitju@yahoo.co.in, skghosh@chm.vnit.ac.in, Phone no: +(91) 712 2801775, Fax: +(91) 712-2223230/2801357

Abstract

Azapodophyllotoxin is a new class of anti-tumor agent with brilliant therapeutic activity and understanding its physicochemical nature in bio-mimetic microenvironments may provide substantial importance in context of its intercellular localization, efficacy as well as delivery. The present work epitomizes environment-sensitive fluorescence modulation of a prodigy, 4-(2-Hydroxyethyl)-10-phenyl-3,4,6,7,8,10- hexahydro-1H-cyclopenta[g]furo[3,4-b]quinoline-1-one (HPFQ) from the class of anti-cancer agent Azapodophyllotoxin, in differently charged model bio-mimetic micellar microenvironment of cationic CTAB, anionic SDS and neutral Triton X-100 using UV-visible absorption, steady state fluorescence, time-resolved fluorescence and fluorescence anisotropy studies. As a distinct phenomenon, anticancer HPFQ exhibits prolific fluorescence in solvents of varying polarity, originating from a mixed contribution of locally excited, charge transfer and excimer emission. A dramatic modulation in the photophysics of HPFQ has been observed in two types of surfactant consortiums: pre-micellar and post-micellar at physiological and anoxic pH. On photo-excitation, anti-cancer HPFQ exists in monomer-excimer equilibrium with varying ratios in different polarity regions. The marked enhancement in fluorescence intensity of HPFQ in post-micellar region of the surfactant under study probably arises due to regeneration of the monomer from its excimer. This reoccurrence reduces the possibility of Förster resonance energy transfer (FRET) from monomer to excimer, which essentially increases the desired emission intensity. Localization of HPFQ in micellar systems highly depends on polarity gradient inside the micelle, electrostatic, hydrophobic and intermolecular hydrogen bonding interactions. Further corroboration with the polarity sensitive experiments in dioxane-water mixture indicates towards spatial localization of the probe molecule in the stern layer of cationic CTAB, sheer surface of neutral TX100 and outer Gouy-Chapman layer in anionic SDS micelles. A molecular binary logic gate correlates the dominance of micellization over the polarity factor,

which enhances the fluorescence response of HPFQ. The enhancement of the emissive potential of anti-cancer HPFQ in biomimetic environments by switching its excimer population may have an immense importance to achieve the status of a dual therapeutic and imaging agent altogether in progressive biomedical research.

Keywords: Azapodophyllotoxin, Micelles, FRET, Time-resolved Fluorescence, Fluorescence Anisotropy.

1. INTRODUCTION

Azapodophyllotoxin, an alternative scaffold to podophyllotoxin, has proved to be an intriguing class of compound coming from intensive research over the years, that was aimed at producing a compound with better anti-proliferative cancer cells, meanwhile maintaining lesser toxicity towards normal living cells. Podophyllotoxin, an antimitotic cyclolignan sequestered from plants of the species *Podophyllumpelatum* L. and *Podophyllumemodi L* [1], was extensively investigated as an anti-tumor compound, but severe gastrointestinal side effects led to disappointing clinical results [2]. Podophyllotoxin has been recognized to possess anti-tumor activity and is still considered an important precursor for research and further development of novel antineoplastic compounds. Consequently, etopophos, etoposide, teniposide etc were derived from podophyllotoxin, and are currently used in clinics for the treatment of diversified malignancies [3–5]. Sometimes, these drugs paved the way for combination therapies with other drugs for improved efficacy. These antineoplastic therapeutics effectively block DNA topoisomerase II and have been frequently used to treat refractory testicular, cell lung, pancreatic and stomach cancers, as well as myeloid leukemias [6,7]. It is believed that, core structure of podophyllotoxin possesses a dual mode of action for its anti-cancer activity: i) inhibition of DNA topoisomerase II and ii) resisting the

formation of microtubule assembly through its binding to tubulin [8]. As ever-evolving cancer cells gradually build up resistance towards the drug used in modern treatments, beside the severe side effects associated with the use of these drugs in clinic; the quest for novel and more effective anticancer analogues of podophyllotoxin still proves to be an extensive area of research.

Derivatives of N-hydroxyethyl-4-aza-didehyropodophyllotoxin displayed brilliant anti-cancer activities against 60 human tumor cell lines with lesser side effects, which provides a wide therapeutic window for potential anticancer application of this class of compound [9]. Interestingly, despite the convenient and uncomplicated synthesis of 4-azapodophyllotoxins, no more further studies of optical properties of Azapodophyllotoxin molecules in biological or bio-mimicking systems have been reported. So, we have taken up the structurally simplest Azapodophyllotoxin derivative (HPFQ) for studying its photo-physical behavior in bio-mimetic micellar systems. HPFQ has proved to be highly active against most cancer cell lines with GI_{50} values of < 0.1µM for 50% cell lines and 0.01 µM for 30% cell lines (encouraging LC_{50} values> 25 µM) [5]. HPFQ has also shown moderate and favorable binding interaction with the carrier proteins human serum albumin (HSA) and bovine serum albumin (BSA), which makes it a favorable agent to be carried throughout the body without much perturbation in protein structure [10,11].

For last two decades, the fluorescence techniques dominated over other optical methodologies to investigate the interaction between probe and natural systems, for its far superior signal-to-noise ratio, even in low temperature experiments. For many years, visualization of interaction between drug molecules and biological systems have depended upon fluorescence detection and subsequently, the use of co-stains, that would generally increase the range of addressable systems and molecules beyond the limitation of their fluorescence capabilities. Usual labelling may also result in perturbation of the investigated

system, as the molecules used for efficient light absorbing and emitting, are frequently larger than the therapeutic probes to which they are attached. Treating the cancer cells without depending upon fluorescence emission from the co-stains for the sake of imaging, may lead to prolonged investigations of potential dual active drug molecules, their activities and structural dynamics. So, we can find such potential molecules towards the demonstration of label-free imaging practices, and to challenge the currently vindicated dominant role of co-stains or labelling in tracking the interaction of drug molecule with non-fluorescing biological systems [12].

In the present article, we have exploited micellar systems (with different charged head groups) to investigate the bioactive molecule because of their ability to closely resemble the structure of cell membranes [13–15]. The diffusion of probe molecule inside micellar structure may amend its photophysical properties because, micelles provide nonpolar-polar interfaces where absorption and emission characteristics of probe molecule becomes enhanced or quenched [16]. Charges on micellar structure may also cast an influence on the optical properties and localization of probe inside micellar system [17,18]. The micelles also carry paramount importance in pharmacy, especially with their ability to solubilize hydrophobic drugs, while assisting towards a control over wetting, stability, bioavailability etc [19–25].

In this work, we provide an assessment of micellar solubilization of HPFQ in surfactant systems bearing different kind of charges, blending it with basic information on modification of optical properties of HPFQ, as well as the localization of drug molecule. Hence, a conspicuous effort has been made to not only provide valuable information for appropriately understanding the spectral characteristic of the HPFQ in a cell-like environment using neutral micelle, cationic micelle and anionic micelle, but also illustrate its binding strategy inside each kind of micellar medium and its location at the molecular level; using UV-visible

absorbance, steady-state fluorescence emission, time resolve fluorescence decay studies, fluorescence anisotropy, steady-state fluorescence quenching and time resolved fluorescence quenching techniques.

2. Experimental Section

2.1 Materials:

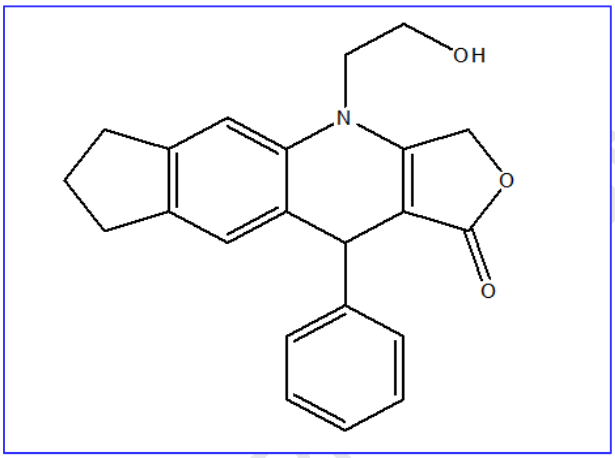

Scheme 1: Structure of HPFQ Molecule

HPFQ [4-(2-Hydroxyethyl)-10-phenyl-3,4,6,7,8,10-hexahydro-1H-cyclopenta[g]furo[3,4-b]quinoline-1-one] was synthesized following the reaction scheme (ESI Scheme S1) and procured in purest form [4]. The spectroscopic grade surfactants cationic cetyl trimethyl ammonium bromide (CTAB) and neutral Triton X-100 (TX-100) were acquired from Sigma-Aldrich chemicals, India. Sodium Dodecyl Sulfate (SDS) was obtained from Alfa Aesar, England. All the surfactants were used without further modification.

2.2 Instrumentation

2.2.1 Steady state absorption and fluorescence emission measurement Steady state absorption measurements were performed at temperature of 298 K with V-630 Spectrophotometer (made by JASCO), operational with Peltier accessories. The JASCO FP-8300 spectrofluorometer, armed with temperature controller unit, was used to record steady state fluorescence spectra. All the measurements were performed using quartz cells of path

length 1.0 cm, while external slit width was kept at 2.5 nm. An excitation wavelength was chosen for HPFQ, which corresponds to the lowest energy band of HPFQ in respective solutions. The background correction was performed by subtracting the appropriate blank.

2.2.2 Steady state Fluorescence anisotropy measurements The JASCO FP-8300 spectrofluorometer, equipped with polarizer accessories, was used to carry out the steady state fluorescence anisotropy experiment. Both the bandwidths for excitation and emission were set at 2.5 nm, for the measurement. The steady state fluorescence anisotropy is calculated by using the following equation [26]:

$$r = (I_{VV} — GI_{VH})/(I_{VV}+2GI_{VH})$$

Here, I_{VV} and I_{VH} correspond to the emission intensities obtained with the excitation polarizer oriented vertically and the emission polarizer oriented vertically and horizontally, respectively. The factor G corresponds to I_{HV}/I_{HH}.

2.2.3Time-resolved fluorescence (TCSPC) Measurements Time-resolved fluorescence (TRF) experiments were performed using a PTI-HORIBA (USA) Picomaster time-resolved spectrofluorometer by time correlated single photon counting (TCSPC) method. A picosecond diode laser of 340 nm was exploited as a source of light for micelle-drug interaction experiments (PTI LED). The PTI light-emitting diode had a pulse width in the range of 700-1100 ps, whereas the response time of PMD-2 detector was approx. 180 ps. The significant design was able to provide us with an undeviating response covering the whole area of photocathode. The detector had an emission spectral range of 185-820 nm. The data were analyzed using 'FelixGX 4.1.2 analysis software' provided by PTI-Horiba (USA). The reduced χ^2 criterion and investigation of the randomness of the fitted function to the raw data led to validation of exponential fittings. The average excited state lifetime $<\tau>$for multi-exponential decay was calculated using decay times $<\tau_i>$ and the relative contribution of components $<a_i>$ in following equation [26]:

$$<\tau>=\sum\tau_i a_i/\sum a_i$$

All the experiments were performed in repetitive manner, until the obtained results were reproduced.

2.3 Sample Preparation

1,4-dioxane of the spectroscopic-grade was used to prepare concentrated stock solution of HPFQ. 10 μL of that stock solution was subsequently added to 2 ml of millipore water for the measurement. The molar extinction coefficient of HPFQ in dioxane is 1.99 x 10^4 L mol^{-1} cm^{-1} (at 319nm). All the solutions were prepared using Millipore water. To obtain hypoxic and anoxic conditions, the pH was adjusted accordingly (5.6 and 7.4). During all the experiments, a positive pressure of nitrogen was maintained to eliminate oxygen. Deoxygenation was put on hold, only at the time of recording absorption and emission spectra. The required quantities of CTAB, SDS and TX-100 were dissolved separately in millipore water of required pH values (7.4 and 5.6), in order to obtain stock solutions of different surfactants.

3. RESULTS AND DISCUSSION:

3.1 A brief revisit to solvent-sensitive behavior of HPFQ

HPFQ exhibits a broad unstructured absorption spectra in water (both at pH 7.4 and 5.6) with an absorption maxima at 327 nm (depicted in Figure 1). On photo-excitation at its absorption maxima, HPFQ exhibits intense fluorescence maxima at 423 nm with a shoulder at 535 nm, in water at pH 7.4 as well as pH 5.6 both in anoxic and hypoxic environment (Figure 1).

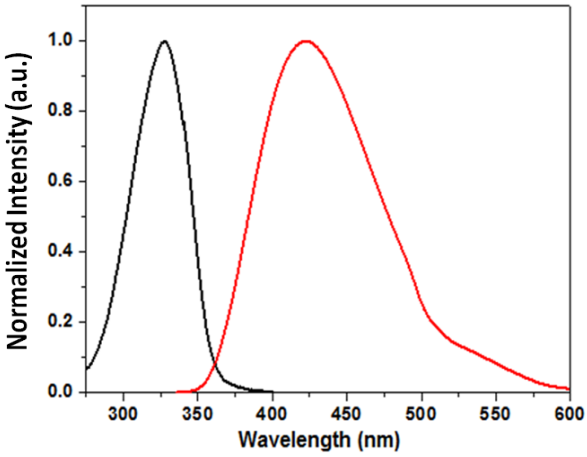

Figure 1: Normalized Absorption (Black) and Emission (Red) spectra of HPFQ ($5.065X10^{-6}$ M) in water at 298 K.

The electronic absorption spectra of HPFQ shows a single absorption band at 327 nm in water, which shows gradual blue shift (~ 12 nm) with decrease in polarity of the solvent and appears at 315 nm in cyclohexane (ESI Table S1) [27]. The fluorescence maxima of HPFQ, while exciting at its absorption maxima, also exhibit a gradual blue shift of 42 nm with the decrease in polarity- from 423 nm in water to 381 nm in cyclohexane (ESI Figure S1), possibly due to a lower extent of charge delocalization in non-polar environment. However, the extent of blue shift in emission spectrum is more appreciable than that of absorption spectrum, which signifies that, the excited state of HPFQ is more sensitive to change in polarity of environment than its ground state.

In the emission profile of HPFQ, a prominent “shoulder” at 535 nm, in addition to its primary emission maxima, has been observed in water. In water, the primary emission maxima at 423 nm is attributed to monomeric form of HPFQ, whereas the shoulder at 535 nm possibly corresponds to the formation of excimer [27]. To identify, whether the formed excimer is static or dynamic one, excitation spectra of HPFQ has been monitored carefully. The similarity in excitation spectra, while monitored at monomer and excimer emission peak individually, eliminates the possibility of static excimer. Moreover, the higher manifestation of excimer peak, when excited at normal absorption peak (328 nm) than exciting selectively

at excimer photo-absorption peak (454 nm) (obtained from excitation spectra acquired at excimer emission band) demonstrates the existence of interesting phenomena of Fröster Resonance Energy Transfer (FRET) from HPFQ monomer to its excimer. The significant overlap between monomer (donor) emission and excimer (acceptor) absorption profiles establishes the aforesaid idea of FRET in a corroborative manner [27]. Throughout the entire polarity scale, HPFQ exhibits appreciable fluorescence, which stems from a mixed contribution of locally excited state, charge transfer state and excimer emission. On photo-excitation, the monomer-excimer ratio of HPFQ keeps dwindling with the change in surrounding polarity and subsequently, the higher population of monomer species has been found to lead to higher emission intensity for HPFQ. Since, the population of HPFQ monomers may have direct influence on the fluorescing capability of therapeutic HPFQ, it will be interesting to monitor the modulation of monomer-excimer population in biomimicking micellar microenvironment having diverse polarity region.

3.2 Decoding the spectral features of HPFQ in different micellar microenvironment

The absorption and fluorescence emission experiments efficiently assist to characterize the micellar organizations because of their intrinsic and non-invasive sensitivity [28]. Consequently, the variations in steady state absorption and emission profiles of HPFQ are investigated in order to decipher the modulation in physicochemical nature of this anti-tumor agent in differently charged model bio-mimetic micellar microenvironment of cationic CTAB, anionic SDS and non-ionic TX-100. All the probe-micelle interactions were monitored at physiological pH of 7.4, as well as hypoxic pH of 5.6 (to replicate acidic nature of solid tumor cells), demonstrating similar results unless stated otherwise.

In aqueous solution of HPFQ, the gradual increase of surfactant concentration imparts spectral variation, in both absorption (ESI Figure S2) and emission (Figure 2), throughout the tested concentration range. The relatively miniscule change in the absorption spectra of

HPFQ indicates that the ground state of the molecule is probably less sensitive towards surrounding micropolarity. The small blue shift (maximum 3 nm, 328 nm to 325 nm, through the considered concentration range in micellar media) observed in absorption spectra (ESI Figure S2) of micellized system may be attributed to reduced delocalization of charge of HPFQ at lesser polar region and therefore diminishing the intermolecular H-bonding interaction. However, the fluorescence spectra of HPFQ shows an appreciable sensitivity towards the micropolarity and the micellization, in terms of better response in fluorescence intensity and shift (Figure 2).

In pre-micellar region, the hydrophobicity that is induced by the interaction between surfactant and HPFQ molecules diminishes the charge redistribution within the molecular framework and therefore a decrease in fluorescence intensity is observed. On gradual addition of surfactant concentration, an increment in emission intensity is observed with appreciable hypsochromic shift of emission maxima in CTAB (423nm to 409nm), SDS (423nm to 414nm) and TX100 (423nm to 411nm). The increase in fluorescence emission intensity starts around critical micellar concentration (CMC) of surfactant due to charge relocalization in excited state of HPFQ by the micellar environment. The micellization increases the probability of ICT within the HPFQ molecular structure. Such phenomena resists diffusion of ground state fluorophore towards an excited fluorophore to form excimers, and thus increasing the fluorescence intensity significantly by favoring the dominance of monomers. Interestingly, the emission intensity shows a minor decrement in post-micellar region due to equilibrium re-distribution of the molecule in micellar and aqueous environment, and stabilization of the HPFQ molecules towards relative non-polar region. Here, the excimer preference by HPFQ in non-polar region plays a part over the monomer formation due to micellization (discussed *vide infra*).

As divulged earlier, HPFQ shows a significant blue shift in its emission maxima on decreasing polarity from polar water to non-polar cyclohexane. HPFQ shows similar hypsochromism in fully micellized solution which strongly indicates its localization in comparatively less polar region than bulk aqueous medium. The extent of hypsochromism of HPFQ, when compared in differently charged micellar systems follows the order CTAB > TX100 > SDS, may indicate the localization of the probe molecule in different location for differently charged micellar medium as micelles help to manifest different polarity regions by virtue of their nature to act as different polarity gradient. The maximum blue shift in CTAB micelle may establish the fact that HPFQ is buried in comparatively more nonpolar region in CTAB than other two micelles.

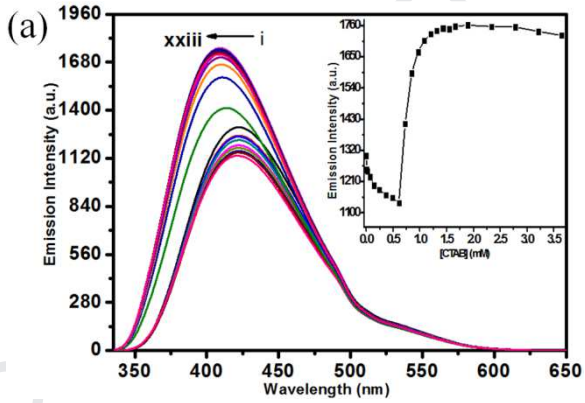

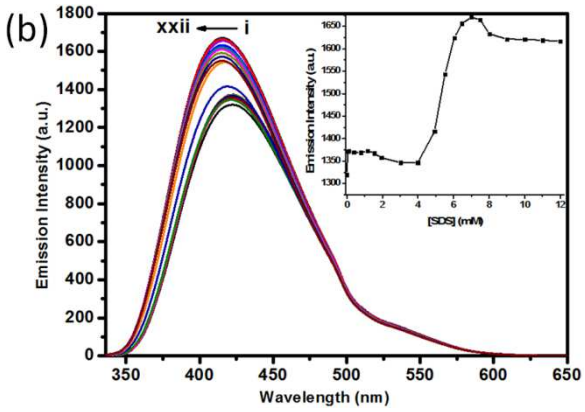

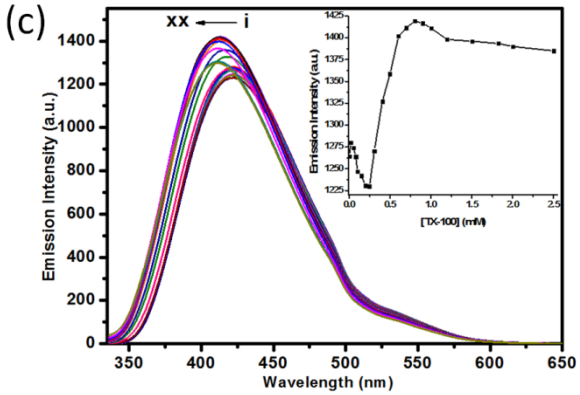

Figure 2: Fluorescence Emission spectra of HPFQ with (a) increasing concentration of CTAB (i to xxiii: 0 mM to 3.645 mM) at 298 K.; (b) increasing concentration of SDS (i to xxii: 0 mM to 13 mM) at 298 K; (c) increasing concentration of TX-100 (i to xx: 0 mM to 2.75 mM) at 298 K. The inset shows the change in emission intensity with the increase in respective surfactant concentration.

The larger hypsochromic shift (14 nm), observed in emission spectra of HPFQ, in CTAB micelle may be attributed due to the strong electrostatic attraction between the non-bonded electrons of the probe molecule and positively charged CTAB surfactant molecules. Such an interaction essentially helps the probe to move more easily towards the non-polar region of CTAB micelle. On the other hand, the greater fluorescence intensity in CTAB micelles may be attributed to better solubilization of HPFQ molecule in cationic micelles by virtue of electrostatic attraction [29]. The relatively weaker interaction between probe and neutral TX-100 surfactant molecule and, a plausible hydrogen bonding interaction between hydrophilic -OH head groups of TX-100 and probe molecule (*vide infra*) might have placed it towards a relatively more polar region in TX-100 micelle than that of the case in CTAB micelle, which depicts a relatively lower extent of hypsochromic shift in TX-100 than CTAB micelle. The electrostatic repulsion between the non-bonded electrons of the probe and negatively charged SDS surfactant molecule is probably the reason behind the lesser interaction, leading to least extent of hypsochromic shift (9 nm), observed in SDS micelle.

In all the three surfactants, there exists a band at 535nm, which attributes to the formation of excimer for the compound (as discussed earlier), in non-polar region. The excimer formation is more favored when the probe resides in relatively non-polar region than the polar aqueous region, which is in line with its photophysical findings, derived from the solvatochromism studies. The excimer emission characteristic is believed to be associated with FRET mechanism, where the absorption by excimer happens from the emission of monomer at 422 nm. In micellized system, the probe tends to move towards non-polar core, so an increase in excimer population was expected, which has been substantiated from TRF studies. But, the formation of HPFQ excimer reduces drastically, which implies a decrease in population of such molecular systems in the excited state, that can accept those FRET energy provided by the locally excited monomer HPFQ molecules (Figure 3). So, despite of increase in donor entities, i.e., monomer population, the excimer formation comes to a halt, owing to micellar entrapment of HPFQ molecules.

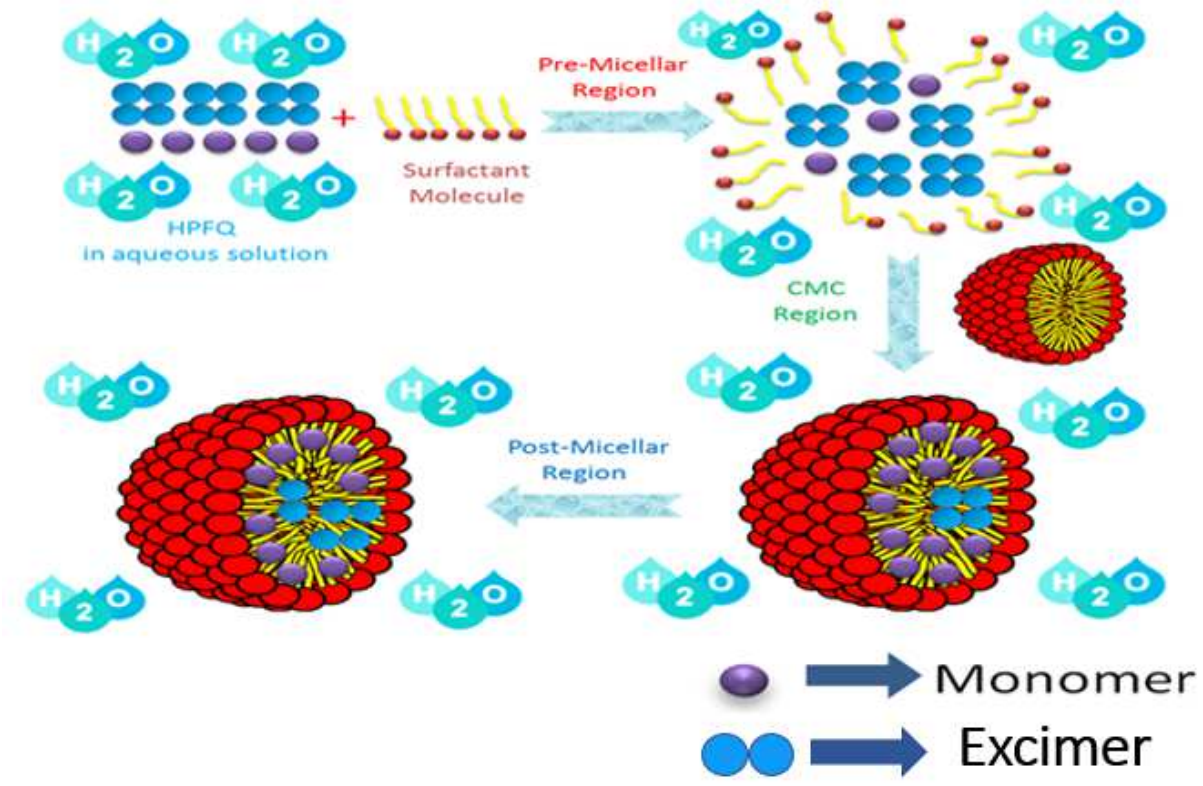

Figure 3: Inter conversion between monomer and excimer of HPFQ molecule with the change in micellar concentration region. The figure demonstrates dramatic decrease in excimer population of HPFQ beyond CMC region.

On the other hand, we can conclude that this compound does not form any kind of static excimer, as the excitation spectra (ESI Figure S3) of the monomer emission maxima and excimer emission maxima overlaps with each other and no subsequent shift was observed along the way [30].

Although, a minute increase in intensity of excimer is observed from emission spectrum, the TRF studies confirms a negligible increase in lifetime of the excimer due to the movement of probe towards non-polar core, which will be discussed in relevant section. So, the compound possesses a substantial preference for its monomer component over the excimer one, in micellized system, which is favorable from the point of better fluorescence response and imaging potential. Furthermore, the observed blue shift of emission maxima in micellar microenvironment may be ascribed to localization of the probe molecule towards relatively non-polar region of the micellar microenvironment, as supported by time resolve fluorescence (TRF), fluorescence anisotropy and fluorescence quenching studies, discussed in following sections.

3.3 Deciphering the Internalization pattern of HPFQ molecule:

Micelles generally possess an anisotropic distribution of water within their structure. Therefore, the concentration of water gradually decreases from the spherical surface of the micelle towards the core of the micellar structure, with an entirely hydrophobic core. Accordingly, the spatial location of a solubilized molecule in a micelle will effectively depend on the polarity of the agent under investigation: nonpolar molecules are solubilized in the micellar core, while substances with intermediate polarity are

found to be distributed in certain intermediate positions, along the surfactant molecules [18].

Therefore, the location of probe inside micelles carries paramount importance, particularly with respect to their capability of solubilizing hydrophobic molecules [31]. In this present section, we have made an effort to provide an overview of micellar solubilization of drugs in different micellar microenvironment.

3.3.1 Identification of the polarity index for the localized region of HPFQ molecule:

The spectral characteristics of a fluorophore in bio-mimicking systems such as micelles, reverse micelles, lipids and proteins are generally compared with its spectra in familiar solvents of predetermined polarity, in order to expose the micropolarity at the vicinity of the fluorophore [32]. The empirical solvent polarity parameter $E_T(30)$ caters as a quantitative parameter for the estimation of micropolarity around the molecule in biphasic environment [33,34]. A graded series of dioxane–water mixture with varying $E_T(30)$ values has been extensively used to satisfy this intention [35,36]. Taking a lead from these facts, the absorption (ESI Figure S4) and emission profile (Figure 4) of HPFQ have been monitored in this graded series of dioxane–water mixtures with known $E_T(30)$ values [35]. The fluorescence emission profile of HPFQ in different dioxane-water mixtures is demonstrated in figure 4. The fluorescence emission band of HPFQ gets blue shifted with increase in percentage of dioxane (i.e. decreasing polarity) in the dioxane-water mixture.

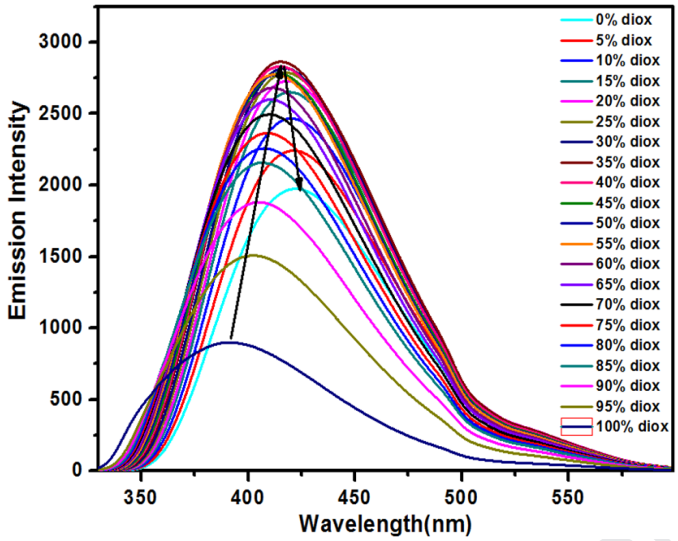

Figure 4: Variation in Fluorescence Emission spectra of HPFQ with increase in percentage of water in water-dioxane mixture at 298 K.

The variation of stokes shift shows a linear trend upto a certain value of $E_T(30)$ (ESI Figure S5). With the addition of 5% water in the HPFQ-dioxane system, the effect of H-bonding in terms of both strength and at inducing ICT to a greater extent starts to become prominent when most of HPFQ molecules fluoresce more efficiently, attributed to the monomer species. When the volume fraction of water in the mixture gets higher (60% water or when $E_T(30)$ = 55.8 kcal/mol, the fluorescence emission intensity of HPFQ reaches a maximum. Thus, a threshold is reached when $E_T(30)$ = 56.6 kcal/mol (ESI Figure S6) or when the binary mixture composed of~65% water fraction, after which a gradual decrement in the fluorescence emission intensity yields a bell shaped curve. At this point it can be stated that the stabilization of the ICT state is very susceptible to the change in polarity of the medium up to the certain extent, after that the sensitivity towards polarity decreases may be due to the fact that the extent of stabilization due to specific interactions e.g, hydrogen bonding, becomes progressively less important with increment of the water concentration in dioxane-water mixture. When the emission intensity was plotted against $E_T(30)$ values, there is a subsequent rise in the emission with increasing polarity followed by a concomitant decrease

366 with further increase in the polarity. This disposition can be accounted in terms of
367 progressive stabilization of the excited state resulting into red shift of the emission band
368 maximum and an increase in fluorescence quantum yield. After certain critical concentration
369 of water (~55%) in the mixture, the ICT state gets further stabilized due to solvation and
370 comes closer to the nearby triplet, giving way to non-radiative decay channels to operate.
371 This observation is used to determine the location of the probe in different surfactants under
372 fully micellized condition. This ensures that the probe is located in less polar region inside
373 the micelles, which can be related with its steady state absorption and fluorescence emission
374 studies.

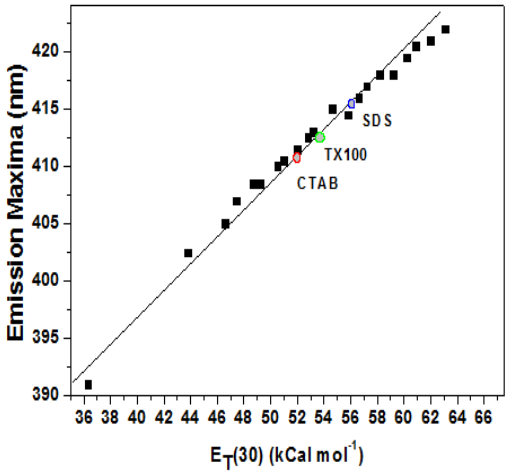

375

376 **Figure 5**: Determination of Probable micropolarity of bound HPFQ in different micellar
377 microenvironment

378 With the help of this experiment, we can determine the equivalency of polarity inside a
379 micelle, where the probe is residing at, with a certain $E_T(30)$ value [37]. The observation
380 (Figure 5) substantiates the claim that (comparing $E_T(30)$ values), the respective polarity of
381 the location of probe inside the CTAB, TX100 and SDS and confirms that the HPFQ is
382 buried deepest inside CTAB micelle and gradually move towards relatively polar location
383 inside TX-100 and SDS respectively.

384 **3.3.2 Measuring the accessibility of HPFQ molecule by the quencher metal ion**

The fluorescence quenching experiment has been used to determine the location of the molecule in three different competing regions inside the micellar system *i.e.* aqueous bulk phase, interfacial region and buried nonpolar core region of the micelles. In fluorescence quenching, the availability of quencher to the fluorophore is extremely necessary as both, dynamic and static quenching require the two interacting partners to come in molecular contact [26]. Thus, the fluorescence quenching experiments of HPFQ in fully micellized systems of all three surfactants have been performed by exploiting Cu^{2+} ion as a quencher (ESI Figure S7). The quencher ion is frequently available in aqueous phase as well as in the micelle–water interface [38],but not to the micellar core, due to very low polarity in the region and thus prompted to the selection of Cu^{2+} as a quencher [39]. Moreover, the fluorescence emission arising from the solution in a fluorescence quenching experiment containing HPFQ and Cu^{2+} comes exclusively from the micelle containing excited fluorophores i.e. from the "photo- selected" population [33,40]. The quenching efficiency of HPFQ by Cu^{2+} in all three different micellar media is quantified by well recognized Stern–Volmer equation:

$$\frac{F_0}{F} = 1 + K_{sv}[Q] = 1 + \mathrm{k_q}\tau\,[\mathrm{Q}]$$

Where, F_0 and F are the fluorescence intensity of HPFQ in absence and presence of quencher and K_{SV} is Stern–Volmer constant, k_q is bimolecular quenching rate constant, τ is average lifetime of fluorophore, [Q] is the concentration of Cu^{2+}. The obtained K_{SV} and k_q values in non-ionic and ionic micelles appear to follow the order SDS > TX-100> CTAB (Table 1)

Table 1. Values of K_{sv} and k_q of HPFQ in aqueous and different surfactant solutions

Surfactant	**K_{sv} (L mol^{-1})**	**k_q (L mol^{-1}s^{-1})**
Water	2.89×10^{3}	9.09×10^{11}

SDS (15 mM)	2.94×10^{5}	7.68×10^{13}
TX100 (2 mM)	2.95×10^{3}	6.94×10^{11}
CTAB (4 mM)	1.41×10^{3}	3.03×10^{11}

406

407 The higher values of K_{SV} is in the order of 10^{5-3} and thus the estimated k_q value at
408 298K is found to be in the order of 10^{11-13} , which is much greater than the
409 maximum possible value of k_q for diffusion controlled quenching (*i.e.*,2.0×10^{10} L
410 $mol^{-1}s^{-1}$) [41,42]. Hence, it may be suggested that the interaction between the
411 cationic quencher ion Cu^{2+} and the negative charge cloud over O-atoms of HPFQ in
412 all these three micellar medium and in aqueous solution is probably static in nature.
413 Static quenching process characteristically produces changes in the absorption
414 profile of probe-quencher interaction, however, such case was not observed for the
415 HPFQ. The anomaly visualized in this study can be explained as follows, the well
416 shielded probe inside the micellar structure is not accessible for dynamic or
417 collisional quenching. While considering this factor and the Stern-Volmer constants
418 obtained in our study, we may assume that the fluorescence quenching of HPFQ by
419 ionic quencher Cu^{2+} follows a sphere of action static quenching model. This
420 hypothesis indicates that the quencher may be able to form a contact with the
421 fluorophore leading to the formation of non-fluorescent species. This theory is
422 further validated by the observation that there occurs no change in the absorption
423 spectral profile of HPFQ, in the presence of Cu^{2+}quencher [43].
424 The Cu^{2+} ion has diminished the emission intensity of the probe molecule more in
425 SDS micelle with better efficiency as compared to the CTAB and TX-100 micellar
426 systems. This observation may be rationalized by the fact that in SDS micelle the

anionic probe is likely to be present in the outer Gouy–Chapman layer or in the aqueous bulk phase and hereby easily accessible to the cationic quencher ion Cu^{2+}. Whereas in non-ionic TX-100, probe is perhaps located in the shear surface region of the surfactant self-assembly, as the quenching is comparable to that in water and is moderately available to the Cu^{2+} ion resulting lesser quenching efficiency than SDS. This explanation is also in line with the result that obtained in fluorescence anisotropy and polarity sensitive experiment as discussed earlier. On contrary, the insignificant quenching that has been observed for HPFQ in CTAB micelles, gives an indication of electrostatic repulsion between likely charged quencher ion and the cationic micellar head group that reduces the chances of interaction between them. Also, the probe is buried in more non-polar region (stern layer) of CTAB micelle, thus, the quenching process becomes comparatively unfavorable. Hence, the metal ion (Cu^{2+}) quenching experiment suggests that the HPFQ is localized inside the Stern layer of CTAB micelle, in the intermediately polar sheer surface of TX-100and, in the outer Gouy–Chapman layer (or aqueous bulk phase) of SDS micelle predominantly.

Excited state dynamics of micelle bound probe molecule with metal ion: Time resolved fluorescence quenching was carried out using TCSPC technique, to figure out the nature of quenching acting between the quencher and the probe molecule. The presence of quenching interaction at excited state or dynamic quenching of probe by the quencher can be easily determined by this experiment [44,45]. There was no significant change observed in excited state lifetime of the probe in presence of Cu^{2+} quencher in water, cationic CTAB and neutral TX100 solution. This clearly indicates that, static quenching is functioning in the aforesaid solutions. But this scenario changes when it comes to anionic SDS micelle (Figure 6). Upon increasing the concentration of metal quencher upto $1.34x10^{-5}$M, we can observe a decrease

in CT lifetime (4.418 ns to 3.041 ns), as well as in the contribution of CT lifetime (80.8% to 13.89%), in turn an increase in contribution of LE lifetime (19.2% to 86.11%) occurs with not much of significant change in its lifetime value (0.792 ns to 0.861 ns). This indicates the existence of dynamic quenching between the probe and quencher, besides having static quenching functioning between them, as stated earlier. This may be due to high electrostatic attraction of cationic metal quencher ion by anionic polar head group of SDS micelle, which insists the probe, present in its aqueous bulk phase, to undergo collisional interaction with quencher ion at the probe's excited state.

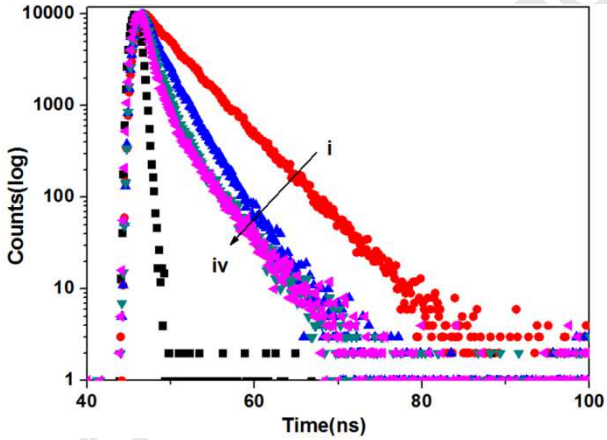

Figure 6: The time resolve fluorescence quenching profile of HPFQ on increasing concentration of Cu^{2+} in SDS (i to iv: 0 µM, 4.5 µM, 13.4 µM and 22.1 µM) surfactant solutions at 298 K.

Influence of low concentration of metal ion on fully micellized HPFQ (in SDS micelle): The following experiment was carried out to provide us enough evidence about the presence of dynamic quenching between the fully SDS micellized probe molecule with bivalent quencher ion Cu^{2+},we carried out fluorescence quenching experiment using very low concentration (starting in 10^{-9} M concentration range) of quencher Cu^{2+} ion. Often we can observe a positive curvature in Stern-Volmer plot, which suggests that, static quenching occurs at high concentration of quencher but at its low concentration, dynamic quenching comes to play [46]. It is believed that the

quenchers, who are only in a sphere of action around fluorophore, at the moment of excitation, come into play [46]. The experiment was carried out to discard all kind of interaction between free cationic quencher ion and free anionic SDS surfactant. Ata very low concentration of quencher ion, all the quencher ions get strongly attracted by micelles only, which lead to its quenching interaction with the micelle-bound probe molecules only. This will subsequently reduce any chance of perturbation arising due to interaction between free surfactant and quencher molecule. Here, a positive deviation was observed in Stern-Volmer plot of F_0/F vs. $[Cu^{2+}]$ (Figure 7), in low concentration range of quencher ion, which may evolve due to strong electrostatic attraction between cationic quencher and anionic surfactant head group. From this deviation in Stern-Volmer plot, we can be ensure that two different types of quenching, i.e, dynamic and static, have been acting between the SDS micelle-bound probe molecule and quencher Cu^{2+} ion. This may attribute to the presence of HPFQ molecule close to anionic head groups of SDS micelles (in outer Gouy-Chapman layer), which facilitates spontaneous interaction between the probe and quencher ions, even at their very low concentrations. Also, this interaction of negative SDS and positive Cu^{2+}quencher, enforces the quencher comes into a closer realm of the probe, that in turn helps in charge transfer between them at the excited state. In the case of CTAB and TX-100 micelles, HPFQ is well shielded in relatively more non-polar region of the micelle and thus, not accessible for dynamic quenching. Again, we can also conclude in a way that the fluorophore located at the exterior or, relatively polar surface can be exposed to dynamic quenching whereas in the interior, higher hydrophobicity may insist the internal fluorophores to be quenched by static process.

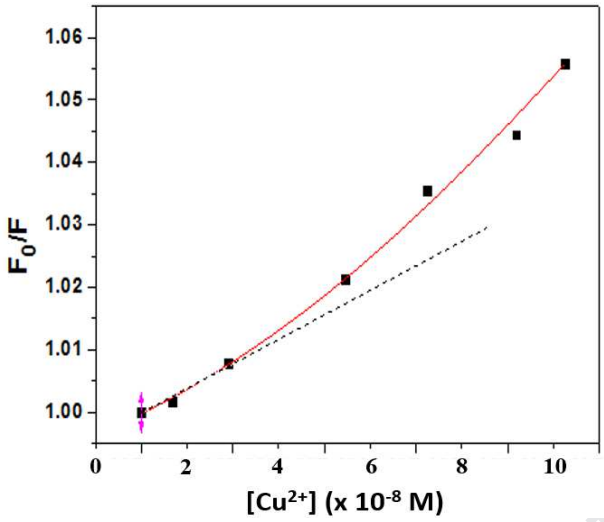

Figure 7: Plot of F_0/F vs. $[Cu^{2+}]$ for determination of quenching nature of HPFQ in anionic SDS solution at 298 K. The positive deviation from linearity is shown by red line. The dotted line represents plausible linear Stern-Volmer plot.

3.3.3 Identification of rotational confinement of HPFQ

Steady state fluorescence anisotropy study has always occupied a position of paramount importance because of its remarkable ability to provide precious information about the microenvironments in the immediate vicinity of the fluorophore [47]. It provides valuable insight about average angular displacement of fluorophore that takes place between absorption and subsequent emission of photon [26]. Hence, it assists to monitor the physical characteristics and the extent of rigidity imposed by the micellar media on the microenvironment of the confined luminophore as compared with unrestricted surrounding of the probe in aqueous medium. Thus, fluorescence anisotropy study of HPFQ has been investigated to get fruitful insight regarding the change in rotational restriction of probe molecule inside micellar environments (Figure 8). In case of CTAB, SDS and TX100, the anisotropy value (*r*) of HPFQ increases with increase in concentration of surfactants and when all probe molecules get confined in fully micellized media, it arrives at a constant value [48,49]. The constant *r* value CTAB, SDS and TX100 micelle is found to be 0.05, 0.03 and 0.09

respectively. The comparatively higher anisotropy values of HPFQ in TX-100 and CTAB micelle strongly indicates, the fluorophore is located in a more confined environment. The relative variation in the *r* values suggests that the probe is located in a more confined state inside TX-100 micellar medium than that in CTAB and SDS.

The fact behind this high *r* value in TX-100 is that, ketonic O atom of HPFQ may form intermolecular hydrogen bonding with H atom of terminal OH group of TX100. So, HPFQ may reside in the sheer surface region of the non-ionic micelle, due to the pull experienced from the terminal –OH group of TX-100. This assumption was validated by temperature dependent quenching studies with HPFQ molecule in fully micellized system of TX-100, which has been discussed in later section.

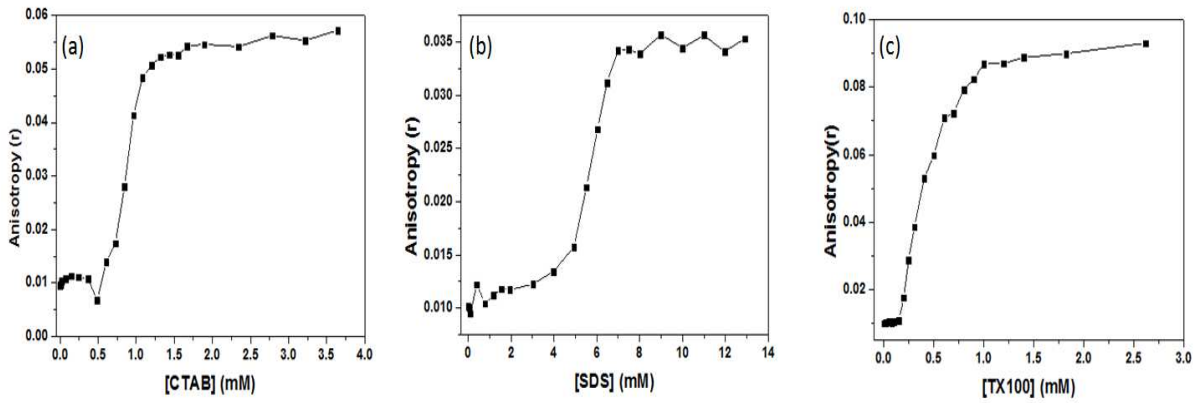

Figure 8: Plot of Fluorescence anisotropy (*r*) vs. concentration of surfactant in case of HPFQ in (a) CTAB, (b) SDS, (c) TX100 surfactant solutions.

In cationic micelle, both hydrophobic and electrostatic interactions come into play for negatively charged fluorophore and therefore, HPFQ orients itself towards inside the Stern layer. However, in anionic micelle due to absence of electrostatic interaction or intermolecular hydrogen bond forces, HPFQ would like to orient itself in the relatively polar outer Gouy-Chapman region of SDS micelle, thus finding itself relatively free from rotational confinement, which attributes to the least *r* value

in SDS micelles. Thus the above result suggests that the HPFQ probe is bound more profoundly with TX-100 as compared to CTAB micelle, plausibly due to presence of intermolecular hydrogen bonding between probe and TX-100. However, in case of SDS, the extent of rotational confinement is diminished because of electrostatic repulsion of the negatively charged fluorophore with anionic SDS micelles.

Effect of temperature on the fluorescence emission profile of TX-bound probe molecule: The temperature dependent fluorescence quenching was carried out for the probe molecule, bound in TX-100 micelle, to figure out the presence of probable intermolecular H-bonding that exists between probe and TX-100 molecule. This intermolecular H-bonding may take place between terminal- OH group of TX-100 and carbonyl O atom of HPFQ (Figure 9).

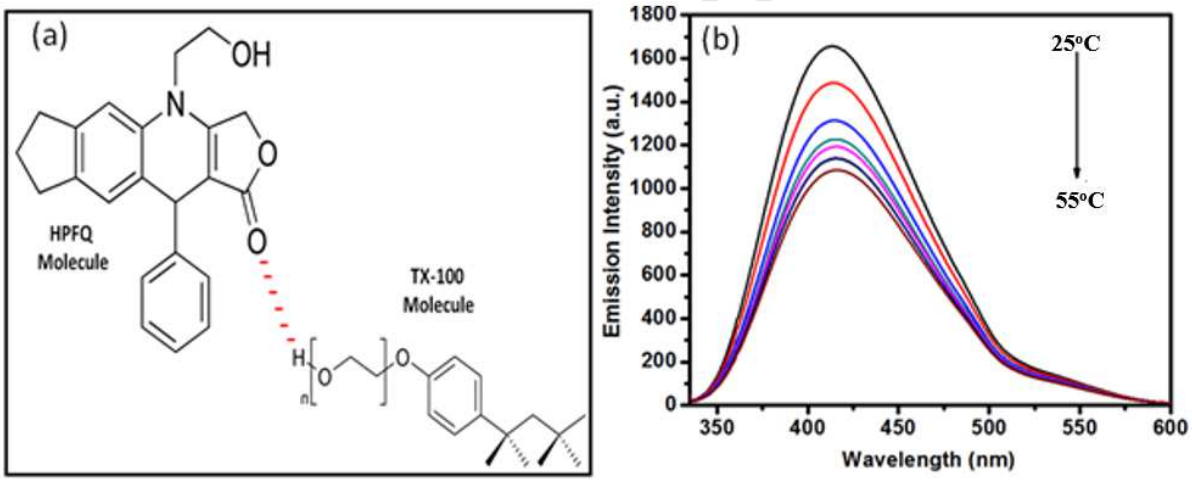

Figure 9: (a) Hydrogen Bonding Interaction observed between terminal –OH group of TX-100 surfactant molecule and carbonyl O atom of HPFQ molecule, (b) Plot of Fluorescence emission intensity vs. wavelength of HPFQ molecule bound in TX-100 micelle at different temperatures (25^0C, 30^0C, 35^0C, 40^0C, 45^0C, 50^0C and 55^0C), confirming hydrogen bonding interaction.

The terminal- OH group, being a part of hydrophilic head group of TX-100, i.e, projected outwards, pulls HPFQ towards the hydrophilic region and thus placing it in the sheer surface of TX-100 micelle. As we increase the temperature, the emission intensity decreases without

any kind of shift in emission maxima. As we know, the CMC of non-ionic micelle decreases with the increase of temperature [50], we carried out the experiment with fully micellar solution at room temperature (Figure 9), which would not be anyhow subjected to destruction of micelle, with rise in temperature. The observed absence of any kind of shift in emission maxima supports this theory. The decrease in emission intensity, can however contribute to, gradual breaking of intermolecular H-bonding with the rise in temperature. Such observation helps us to commemorate the assumption of formation of intermolecular H-bond between TX-100 and probe molecule. Such after-effect was not observed in case of CTAB and SDS surfactant molecules, due to their inability to form H-bond with the HPFQ molecule.

Depicting the Probable location of HPFQ in SDS, CTAB and TX-100 micellar systems: The highest anisotropy value in neutral TX100 micelle may be the consequence of the hydrophobicity and the intermolecular hydrogen due to presence of the probe in the sheer surface of TX-100 micelle. The lowest anisotropy value was found to be in SDS, which may be due to the presence of probe in its outer Gouy-Chapman layer. The lowest quenching was observed in cationic CTAB micelle due to the fact that the probe is buried deep inside the Stern layer of the micelle. The subsequent and other relevant results have also been discussed in relevant places to justify the positions of the probe in different micellar microenvironment (Figure 13).

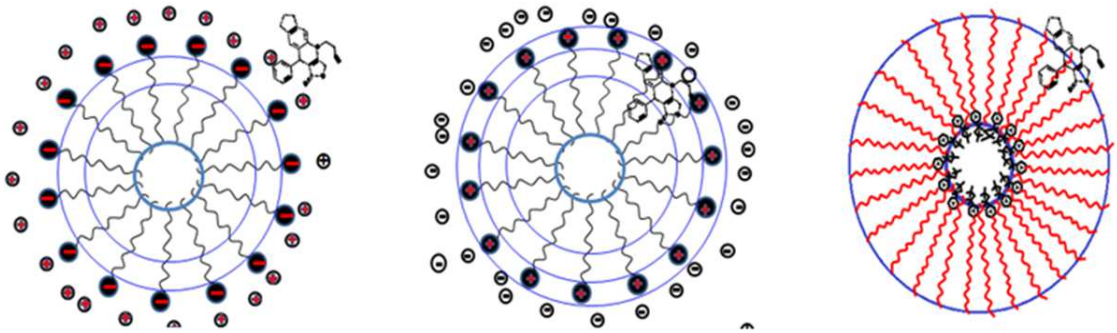

(a) (b) (c)

Scheme 2: Probable localization of HPFQ in (a) anionic SDS, (b) cationic CTAB and (c) neutral TX100 micelles.

3.4 Modulation of monomer-excimer equilibrium dynamics induced by biomimetic systems

The time resolved fluorescence (TRF) study is of great importance to establish ground and excited state interaction between micelle and probe [51]. TRF serves as an indicator, which is extremely sensitive towards even any minute change of local environment around the fluorophore and thus responsive towards the excited state interaction [52]. Differential solvent relaxation around the fluorophore and/or partitioning of the fluorophore in distinct region of a confined environment give rise to differences in the lifetime of the fluorophore [53]. The tendency of this molecule to orient itself in relative non-polar hydrophobic core of micelle was investigated by TRF using time-correlated single photon counting (TCSPC) technique. For each solution, the excitation was carried out using a 340nm LED and the emission was monitored at respective monomer emission maxima.

At first, TRF was studied placing the probe in solvents of different polarity (Figure 10). In all solutions, fluorescence decay profile of HPFQ was found to be best fitted for two component systems. These larger lifetime components is assigned as monomer, while the smaller one as the dynamic excimer state of HPFQ [27]. In polar solvents, the excimer species (τ_1<1 ns) was observed to pose as a minor contributor (α_1~10%) and the long lived monomer species (τ_2~3 ns) as a major contributor (α_2~90%), suggesting the domination of monomer over excimer. But, as soon as we move towards non polar solvents, the excimer state was observed to predominate with a substantial increase in lifetime and contribution over the monomeric form of HPFQ. The build-up of H-bond interaction for HPFQ in polar solvents may be attributed a discrete evidence of dynamic conversion of excimers into monomers [27]. The fluorescence decay profile of HPFQ was studied in aqueous solution and micellar solutions of CTAB, SDS

and TX100 (Figure 11) in order to get further information on the heterogeneous surrounding of the excited probe molecule inside the micellar medium [51]. The fluorescence decay profiles of HPFQ appeared to be well defined by a double exponential fitting, as shown in Table 2. The larger lifetime species (3.399ns, 92.06%) has greater contribution in aqueous solution than the smaller lifetime species (0.701ns, 7.09%). In the premicellar region of all three surfactants, the lifetime of excimer species of HPFQ shows a substantial increase in both lifetime and contribution. The hydrophobicity induced by surfactant molecules on HPFQ encourages formation of aggregate in excited state of HPFQ, subsequently reducing the probability of charge delocalization in molecular framework. At CMC, formation of micellar systems help to disaggregate excimer resulting in reduction of its lifetime and consequently, increases both the lifetime and contribution of the monomer. In CTAB micelles, the lifetime of monomer species (τ_2) increases from 3.399 ns to 4.698 ns. In case of TX100 and SDS micelle, HPFQ shows a similar trend in excited state lifetime, where the lifetime for monomer (τ_2) increases from 2.959 ns to 3.778 ns and from 3.291 ns to 3.977 ns respectively.

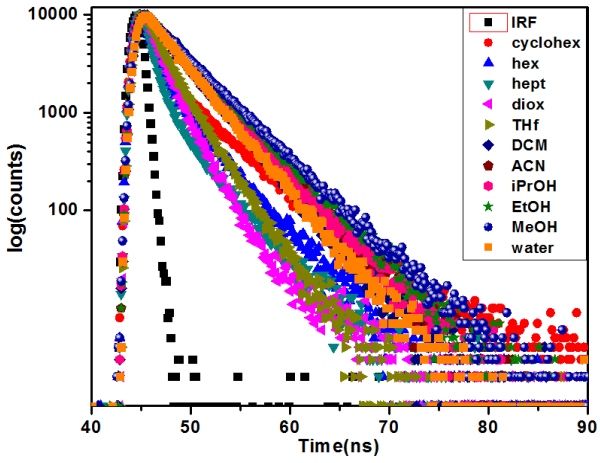

Figure 10: The time resolve fluorescence decay profile of HPFQ in solvents of different polarity at 298 K [27].

In post-micellar region, again the hydrophobicity between HPFQ and surfactant molecules increases, as the HPFQ prefers to orient itself towards non-polar core of micellar systems. As a result, a small increase in contribution and lifetime of excimer is observed. But, owing to

micellization effect, the substantial increase in monomer lifetime overshadows such participation of its excimer counterpart and increases the average lifetime of HPFQ to several decimals. Herein, the triumph of monomer lifetime over the contribution of its excimer enhances the fluorescence response of HPFQ to a higher degree, despite its movement towards non-polar core. Such phenomenon helps to express better fluorescence activity in micellar and post-micellar region of the compound.

Comparatively, larger lifetime of a monomer species in case of CTAB micelle can be justified by its localization inside the micelle, which is buried towards relatively more non-polar region or hydrophobic core of micelle and therefore leading to better solubilization in micellar media. In TX-100 and SDS micelle, the probe resides in relatively more polar region of the micelle, i.e, close to polarity of aqueous region, and hence the lifetime and percentage contribution of monomer increases to a lower degree.

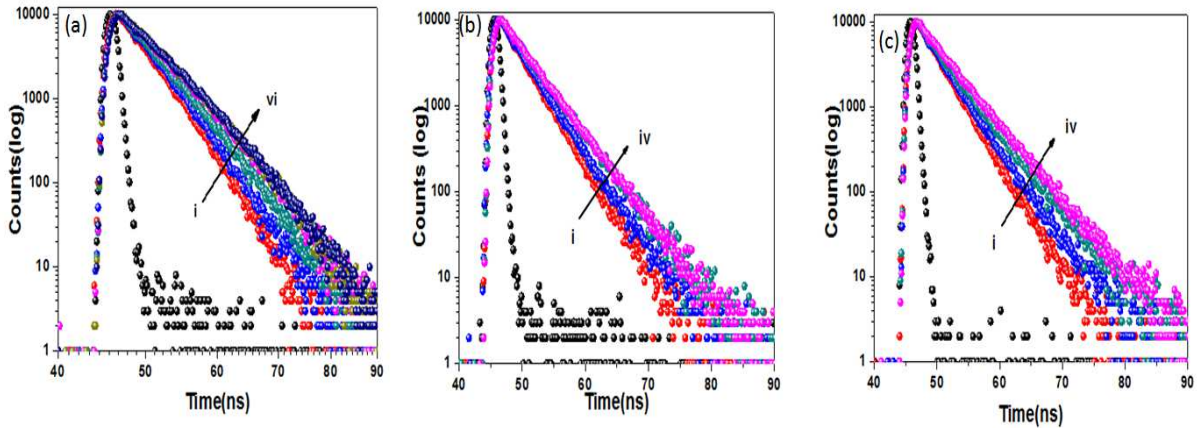

Figure 11: The time resolve fluorescence decay profile of HPFQ in premicellar and postmicellar concentrations of (a) CTAB (i to vi: 0 mM, 0.61 mM, 0.73 mM, 0.96 mM, 1.08 mM and 1.43 mM), (b) SDS (i to iv: 0 mM, 4.94 mM, 6.99 mM and 7.50 mM) and (c) TX100 (i to iv: 0 mM, 0.30 mM, 0.59 mM and 1.38 mM) surfactant solutions at 298 K.

If we closely look at the variation of excited state lifetime, we can note that in pre-micellar region, local concentration of probe molecule is very high in excited state, which induces the formation of excimer. Just after crossing CMC, formation of micellar assembly induces the

disaggregation of local assembly of probe, helping rapid conversion of excimer into monomer, which reflects in higher lifetime and contribution of the monomer at higher concentrations than CMC. Subsequently, this increase in lifetime and contribution of monomer species at micellar system helps to clarify the phenomena of increasing emission intensity, which we observed in previous section.

Table 2. TRF measurement of HPFQ in aqueous and different micellar solutions at 298 K

Environment	τ_1 (ns)	τ_2 (ns)	α_1(%)	α_2(%)	χ^2	Average lifetime (<τ>, ns)
Water	0.701	3.399	7.94	92.06	1.12	3.185
CTAB(0.61mM)	1.624	3.758	13.67	86.33	1.18	3.466
CTAB(1.1mM)	1.475	4.889	5.59	94.41	1.30	4.698
CTAB(1.9mM)	1.295	4.982	9.32	90.68	1.29	4.638
TX100 (0.14mM)	0.364	3.421	15.08	84.92	1.14	2.959
TX100 (0.39mM)	1.925	4.548	29.34	70.66	1.09	3.778
TX100 (1.81mM)	1.466	4.869	17.29	82.71	1.20	4.281
SDS(1.5 mM)	0.951	3.489	7.8	92.2	1.15	3.291
SDS(8.0 mM)	0.875	4.254	8.18	91.82	1.25	3.977
SDS(11.0 mM)	1.151	4.385	8.85	91.15	1.28	4.098

The higher monomer lifetime in different micellar environment and subsequent increase in average lifetime for HPFQ compared to that in pure aqueous medium indicates the dominance of micellization factor in governing the enhanced fluorescence response of the probe, despite its movement towards non-polar region of micelle. Such encouraging observations make HPFQ a suitable candidate for imaging with specific therapeutic interactions.

3.5 An Illustration of 'Competition between polarity and micellization' by molecular logic gate:

From the context of better imaging capability, i.e, enhanced excited state lifetime of HPFQ, we have designed a molecular logic gate, based on 'Boolean Algebra' to demonstrate the dominant factor between polarity and micellar entrapment (Figure 12). Here, the polarity and micellization factors in different stage of micellar assemblies are taken as input, whereas the average excited state lifetime of HPFQ in those conditions were taken as output. We have taken threshold value for average excited state lifetime of HPFQ to be 3.5ns, for an efficient construction of logic gate. In aqueous solution, both the inputs (governing factors) were selected to be zero (0). The corresponding $<\tau>$ for HPFQ was found to be lower than the threshold value, i.e, turning the output to be as an 'OFF' switch (0). In premicellar region, the HPFQ molecule was subjected to hydrophobic interaction with surfactant molecules, without any formation of micelles. So, the polarity factor was taken as 'ON' (input 1) but the micellization factor was 'OFF' (input 0), which gave the output of $<\tau>$ lower than threshold value, thus turning the output as 'OFF' (0). At around critical micellar concentration (CMC), the formation of micellar structure becomes a critical factor to bring in a drastic change of surrounding environment of HPFQ. Accordingly, the input of polarity was taken to be 'OFF' (0) but the micellization factor was taken as 'ON' (1); subsequently output $<\tau>$ was found to be above threshold value and thus output was taken as 'ON' (1). In post-micellar region, both the input was taken as 'ON' (1), as the HPFQ molecule tends to orient itself towards non-polar core of micelles. Subsequent output $<\tau>$, being higher than threshold value, was taken to be 'ON' (1). Thus, we can see, until the polarity remains sole governing factor, the output was taken to be '0'. But, as soon as, micellization comes into play, the $<\tau>$ keeps responding over the decided threshold value and thus turning the excited state lifetime to be 'ON' (1). So, in water and pre-micellar region, the output was taken as 'OFF' (0) and at CMC and post-

micellar region, the output was taken as 'ON' (1). We can observe, only the input sets of (0,1) and (1,1) i.e., when the micellization starts to play a role (in both presence and absence of polarity factor), gave positive response for output over threshold value of excited state lifetime. Such observations led us to forming an explanatory system to demonstrate the dominant factor between polarity and micellization, based on 'BOOLEAN Algebra', ultimate resulting in formation of a complex logic gate using universal 'NAND' gate.

Input (Polarity)	Input (Micellization)	Output (Excited state lifetime)
0	0	0
1	0	0
0	1	1
1	1	1

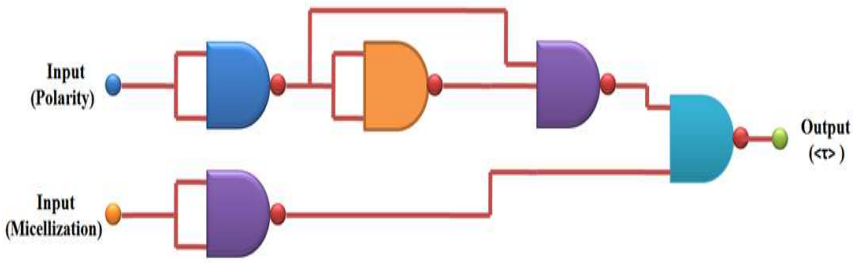

Figure 12: Molecular logic gate and corresponding Truth table for HPFQ in biomimetic environments.

CONCLUSION

HPFQ, the simplest azapodophyllotoxin scaffold, has proved to be a brilliant therapeutic molecule with promising fluorescent properties. In possession of a very rare phenomena, HPFQ chisels its own niche of fluorescing along the entire polarity ambit by the virtue of a combined effect pertained by LE, CT and excimer emission properties. HPFQ exhibits a peculiarity of sustaining in monomer-excimer equilibrium with varying ratios, along the entire polarity region and the phenomenon is well reflected in the micellar systems. HPFQ orients itself inside the Stern layer of CTAB, in sheer surface of TX100 and outer Gouy-Chapman layer of SDS. This foresaid localization of HPFQ in model bio-mimicking systems modulates the regeneration of monomer from its excimer by different extent and ultimately results in the increment of radiative lifetime as compared to that of the bioactive probe in aqueous media, which has further been corroborated with the findings from time resolved

fluorescence studies. Molecular logic gate has been utilized to establish that the micellization overcomes the polarity factor to increase the monomer population and subsequently elevates the fluorescing intensity as well as radiative lifetime of HPFQ in model bio-mimetic environments. The results obtained herewith may inspire the idea of using HPFQ as a potential dual therapeutic and fluorescence imaging agent for cancer treatment in future, where HPFQ may sustain without the help of co-stains to monitor its desired therapeutic intervention. Since the excitation wavelength for HPFQ lies in the UV region (328 nm in water), at present, two or three photon excitation may be of use to promote HPFQ as a simultaneous therapeutic and imaging agent.

Acknowledgements

The authors greatly acknowledge the support from Department of Chemistry, VNIT, Nagpur for access to instruments and other necessary lab facilities. Research reported in this article was partly supported by an Institutional Development Award (IDeA) from the National Institute of General Medical Sciences of the National Institutes of Health under grant number P20 GM103475-14. The content is solely the responsibility of the authors and does not necessarily represent the official views of the National Institutes of Health.

References

[1] N.D. and C. Gm, Natural Products as Sources of New Drugs over the 30 Years, J. Nat. Prod. 75 (2012) 311–335. doi:10.1021/np200906s.Natural.

[2] T.F. Imbert, Discovery of podophyllotoxins, Biochimie. 80 (1998) 207–222. doi:10.1016/S0300-9084(98)80004-7.

[3] A. Kumar, V. Kumar, A.E. Alegria, S.V. Malhotra, Synthetic and Application

Perspectives of Azapodophyllotoxins: Alternative Scaffolds of Podophyllotoxin, Curr Med Chem. 18 (2011) 3853–3870.

[4] A. Kumar, V. Kumar, A.E. Alegria, S. V Malhotra, N-hydroxyethyl-4-aza-didehydropodophyllotoxin derivatives as potential antitumor agents., Eur. J. Pharm. Sci. 44 (2011) 21–6. doi:10.1016/j.ejps.2011.04.013.

[5] A. Kumar, A.E. Alegria, Synthesis of Novel Functionalized 4-Aza-2,3-Didehydropodophyllotoxin Derivatives with Potential Antitumor Activity, J Heterocycl Chem. 47 (2010) 1275–1282. doi:10.1002/jhet.467.

[6] W. Ross, T. Rowe, B. Glisson, J. Yalowich, L. Liu, Role of TopoisomeraseII in MediatingEpipodophyllotoxin-induced Ie, 44 (1984) 5857–5860.

[7] B.H. Long, S.T. Musial, M.G. Brattain, DNA Breakage in Human Lung Carcinoma Cells and Nuclei That Are Naturally Sensitive or Resistant to Etoposide and Teniposide1, 213 (1986) 3809–3816.

[8] Ajay Kumar, Vineet Kumar, Antonio E. Alegria, Sanjay V. Malhotra, N-Hydroxyethyl-4-aza-didehydropodophyllotoxin derivatives as potential antitumor agents, Eur. J. Pharm. Sci. 44 (2011) 21–26. doi:10.1016/j.ejps.2011.04.013.

[9] C. Shi, J. Wang, H. Chen, D. Shi, Regioselective Synthesis and in Vitro Anticancer Activity of 4-Aza-podophyllotoxin Derivatives Catalyzed by l -Proline, J. Comb. Chem. 12 (2010) 430–434. doi:10.1021/cc100003c.

[10] S. Mukherjee, K. Ganorkar, A. Kumar, N. Sehra, S.K. Ghosh, Switching of Trp-214 intrinsic rotamer population in human serum albumin: An insight into the aftermath of embracing therapeutic bioorganic luminophore azapodophyllotoxin into sudlow site I, Bioorg. Chem. 84 (2019) 63–75. doi:10.1016/J.BIOORG.2018.11.015.

[11] S. Mukherjee, K. Ganorkar, S. Gupta, A. Kumar, A. Singh, S.K. Ghosh, The consequences of adopting therapeutic luminophore azapodophyllotoxin into BSA: a molecular regulator to control emissive population of two tryptophan residues in carrier protein, J. Biomol. Struct. Dyn. (2019) 1–14. doi:10.1080/07391102.2019.1630320.

[12] J.O. Arroyo, P. Kukura, Non-fluorescent schemes for single-molecule detection, imaging and spectroscopy, Nat. Photonics. 10 (2015) 11–17. doi:10.1038/nphoton.2015.251.

[13] M.E. Haque, A.R. Das, S.P. Moulik, Mixed Micelles of Sodium Deoxycholate and Polyoxyethylene Sorbitan Monooleate (Tween 80), J. Colloid Interface Sci. 217 (1999) 1–7. doi:10.1006/jcis.1999.6267.

[14] A.K. Dwivedi, M. Pandeeswar, T. Govindaraju, Assembly Modulation of PDI Derivative as a Supramolecular Fluorescence Switching Probe for Detection of Cationic Surfactant and Metal Ions in Aqueous Media, ACS Appl. Mater. Interfaces. 6 (2014) 21369–21379. doi:10.1021/am5063844.

[15] N. Sarkar, K. Das, A. Datta, S. Das, K. Bhattacharyya, Solvation Dynamics of Coumarin 480 in Reverse Micelles. Slow Relaxation of Water Molecules, J. Phys. Chem. 100 (1996) 10523–10527. doi:10.1021/jp953658l.

[16] M. Jadhao, R. Joshi, K. Ganorkar, S.K. Ghosh, Biomimetic systems trigger a benzothiazole based molecular switch to ‘turn on’ fluorescence, Spectrochim. Acta Part A Mol. Biomol. Spectrosc. 217 (2019) 197–205. doi:10.1016/J.SAA.2019.03.089.

[17] D.J. McClements, Nanoemulsions versus microemulsions: terminology, differences, and similarities, Soft Matter. 8 (2012) 1719. doi:10.1039/c2sm06903b.

[18] S. Choudhary, N. Kishore, Drug-protein interactions in micellar media: Thermodynamic aspects, J. Colloid Interface Sci. 413 (2014) 118–126. doi:10.1016/j.jcis.2013.09.026.

[19] A. Ganguly, S. Ghosh, N. Guchhait, Modulated photophysics of an anthracene-based fluorophore within bile-salt aggregates: the effect of the ionic strength of the medium on the aggregation behavior, Photochem. Photobiol. Sci. 14 (2015) 2168–2178. doi:10.1039/C5PP00280J.

[20] M. Gaber, T.A. Fayed, S.A. El-Daly, Y.S. El-Sayed, Spectral properties and inclusion of a hetero-chalcone analogue in organized media of micellar solutions and beta-cyclodextrin, Photochem. Photobiol. Sci. 7 (2008) 257–262. doi:10.1039/B713381B.

[21] S. Freire, J. Bordello, D. Granadero, W. Al-Soufi, M. Novo, Role of electrostatic and hydrophobic forces in the interaction of ionic dyes with charged micelles, Photochem. Photobiol. Sci. 9 (2010) 687. doi:10.1039/b9pp00198k.

[22] S.A. Gerhardt, J.W. Lewis, J.Z. Zhang, R. Bonnett, K.A. McManus, Photophysical behaviour of an opp-dibenzoporphyrin (2, 12-diethyl-3,13-dimethyldibenzo[g,q]porphyrin) in micelles and organic solvents, Photochem. Photobiol. Sci. 2 (2003) 934. doi:10.1039/b301637d.

[23] T.S. Singh, S. Mitra, Fluorimetric studies on the binding of 4-(dimethylamino)cinnamic acid with micelles and bovine serum albumin, Photochem. Photobiol. Sci. 7 (2008) 1063. doi:10.1039/b717475f.

[24] C. Carnero Ruiz, Rotational dynamics of coumarin 153 in non-ionic mixed micelles of n-octyl-β-d-thioglucoside and Triton X-100, Photochem. Photobiol. Sci. 11 (2012) 1331. doi:10.1039/c2pp25049g.

[25] E. Rajkumar, P.M. Mareeswaran, S. Rajagopal, Photophysical properties of amphiphilic ruthenium(ii) complexes in micelles, Photochem. Photobiol. Sci. 13 (2014) 1261–1269. doi:10.1039/C4PP00043A.

[26] J.R. Lakowicz, Principles of Fluorescence Spectroscopy | Springer, 2007. http://www.springer.com/us/book/9780387312781.

[27] S.K. Ghosh, R. Joshi, S. Mukherjee, A. Kumar, A. Singh, M. Concepcion-Santana, Unusual Photophysics of Anticancer Azapodophyllotoxin: The Collective Effect of Discrete H-bond Motif Spills the Beans, J. Photochem. Photobiol. A Chem. 349 (2017) 49–62. doi:10.1016/j.jphotochem.2017.08.069.

[28] G.B. Behera, B.K. Mishra, P.K. Behera, M. Panda, Fluorescent probes for structural and distance effect studies in micelles, reversed micelles and microemulsions, Adv. Colloid Interface Sci. 82 (1999) 1–42. doi:10.1016/S0001-8686(98)00086-4.

[29] R. Gomes, A.J. Parola, C.A.T. Laia, F. Pina, Efficient photochromism from the network of chemical reactions of 7,4′-dihydroxyflavylium in CTAB micelles, Photochem. Photobiol. Sci. 6 (2007) 1003. doi:10.1039/b707461a.

[30] A. Ghosh, A. Sengupta, A. Chattopadhyay, D. Das, Lysine triggered ratiometric conversion of dynamic to static excimer of a pyrene derivative: aggregation-induced emission, nanomolar detection and human breast cancer cell (MCF7) imaging, Chem. Commun. 51 (2015) 11455–11458. doi:10.1039/C5CC02389K.

[31] M. Jadhao, S. Mukherjee, R. Joshi, H. Kumar, S.K. Ghosh, Aggregation-disaggregation pattern of photodynamically active ZnPcS 4 and its interaction with DNA alkylating quinone: Effect of micellar compactness and central metal ion, RSC Adv. 6 (2016) 77161–77173. doi:10.1039/c6ra13151d.

[32] S.K. Ghosh, S.C. Bhattacharya, Interaction of 3,7-diamino-2,8-dimethyl-5-phenyl phenazinium chloride with model biological membranes and reverse micelles of lipid: a spectroscopic study, Chem. Phys. Lipids. 131 (2004) 151–158. doi:10.1016/j.chemphyslip.2004.04.010.

[33] S.K. Ghosh, P.K. Khatua, S.C. Bhattacharya, Physicochemical characteristics of reverse micelles of polyoxyethylene nonyl phenol in different organic solvents, J. Colloid Interface Sci. 279 (2004) 523–532. doi:10.1016/j.jcis.2004.06.089.

[34] S.K. Ghosh, S.U. Hossain, S. Bhattacharya, S.C. Bhattacharya, 2-(2-Selenocyanic acid ethyl ester)-1H-benz[de] isoquinoline-1,3-(2H)-dione, synthesis photophysics and interaction with bovine serum albumin: A spectroscopic approach, J. Photochem. Photobiol. B Biol. 81 (2005) 121–128. doi:10.1016/j.jphotobiol.2005.07.004.

[35] E.M. Kosower, H. Dodiuk, K. Tanizawa, M. Ottolenghi, N. Orbach, Intramolecular donor-acceptor systems. Radiative and nonradiative processes for the excited states of 2-N-arylamino-6-naphthalenesulfonates, J. Am. Chem. Soc. 97 (1975) 2167–2178. doi:10.1021/ja00841a030.

[36] A. Mallick, B. Haldar, S. Maiti, S.C. Bera, N. Chattopadhyay, Photophysical Study of 3-Acetyl-4-oxo-6,7-dihydro-12 *H* -indolo[2,3- *a*]quinolizine in Biomimetic Reverse Micellar Nanocavities: A Spectroscopic Approach, J. Phys. Chem. B. 109 (2005) 14675–14682. doi:10.1021/jp050511d.

[37] M. Jadhao, P. Ahirkar, H. Kumar, R. Joshi, O.R. Meitei, S.K. Ghosh, Surfactant induced aggregation–disaggregation of photodynamic active chlorin e6 and its relevant interaction with DNA alkylating quinone in a biomimic micellar microenvironment, RSC Adv. 5 (2015) 81449–81460. doi:10.1039/C5RA16181A.

[38] A. Mallick, B. Haldar, S. Maiti, N. Chattopadhyay, Constrained photophysics of 3-acetyl-4-oxo-6,7-dihydro-12H indolo-[2,3-a] quinolizine in micellar environments: a spectrofluorometric study, J. Colloid Interface Sci. 278 (2004) 215–223. doi:10.1016/j.jcis.2004.05.027.

[39] A. Mahata, D. Sarkar, D. Bose, D. Ghosh, A. Girigoswami, P. Das, N. Chattopadhyay, Photophysics and Rotational Dynamics of a β-Carboline Analogue in Nonionic Micelles: Effect of Variation of Length of the Headgroup and the Tail of the Surfactant, J. Phys. Chem. B. 113 (2009) 7517–7526. doi:10.1021/jp900575e.

[40] M. Almgren, F. Grieser, J.K. Thomas, Dynamic and static aspects of solubilization of neutral arenes in ionic micellar solutions, J. Am. Chem. Soc. 101 (1979) 279–291. doi:10.1021/ja00496a001.

[41] X. Zhao, R. Liu, Z. Chi, Y. Teng, P. Qin, New Insights into the Behavior of Bovine Serum Albumin Adsorbed onto Carbon Nanotubes: Comprehensive Spectroscopic Studies, J. Phys. Chem. B. 114 (2010) 5625–5631. doi:10.1021/jp100903x.

[42] H. Kumar, V. Devaraji, R. Joshi, M. Jadhao, P. Ahirkar, R. Prasath, P. Bhavana, S.K. Ghosh, Antihypertensive activity of a quinoline appended chalcone derivative and its site specific binding interaction with a relevant target carrier protein, RSC Adv. 5 (2015) 65496–65513. doi:10.1039/C5RA08778C.

[43] Y. Rahimi, A. Goulding, S. Shrestha, S. Mirpuri, S.K. Deo, Biochemical and Biophysical Research Communications Mechanism of copper induced fluorescence quenching of red fluorescent protein , DsRed, 370 (2008) 57–61. doi:10.1016/j.bbrc.2008.03.034.

[44] N.A.M. Sultan, M.J. Swamy, Fluorescence quenching and time-resolved fluorescence

studies on Trichosanthes dioica seed lectin, J. Photochem. Photobiol. B Biol. 80 (2005) 93–100. doi:10.1016/j.jphotobiol.2005.03.003.

[45] M.H. Gehlen, F.C. De Schryver, Time-resolved fluorescence quenching in micellar assemblies, Chem. Rev. 93 (1993) 199–221. doi:10.1021/cr00017a010.

[46] J. Keizer, Nonlinear fluorescence quenching and the origin of positive curvature in Stern-Volmer plots, J. Am. Chem. Soc. 105 (1983) 1494–1498. doi:10.1021/ja00344a013.

[47] A. Samanta, B.K. Paul, N. Guchhait, Studies of bio-mimetic medium of ionic and non-ionic micelles by a simple charge transfer fluorescence probe N,N-dimethylaminonapthyl-(acrylo)-nitrile, Spectrochim. Acta Part A Mol. Biomol. Spectrosc. 78 (2011) 1525–1534. doi:10.1016/j.saa.2011.01.044.

[48] S.S. Mati, T.K. Mondal, S. Dhar, S. Chall, S.C. Bhattacharya, Differential contribution of Igepal and CnTAB micelles on the photophysics of nonsteroidal drug Naproxen, Spectrochim. Acta Part A Mol. Biomol. Spectrosc. 92 (2012) 122–130. doi:10.1016/j.saa.2012.02.042.

[49] N.C. Maiti, M.M.G. Krishna, P.J. Britto, N. Periasamy, Fluorescence Dynamics of Dye Probes in Micelles, J. Phys. Chem. B. 101 (1997) 11051–11060. doi:10.1021/jp9723123.

[50] M.J. Schick, Effect of temperature on the critical micelle concentration of nonionic detergents. Thermodynamics of micelle formation, J. Phys. Chem. 67 (1963) 1796–1799. doi:10.1021/j100803a013.

[51] S. Draxler, M.E. Lippitsch, Lifetime-based sensing: influence of the microenvironment., Anal. Chem. 68 (1996) 753–7. doi:10.1021/ac9507092.

[52] A. Maciejewski, D.R. Demmer, D.R. James, A. Safarzadeh-Amiri, R.E. Verrall, R.P. Steer, Relaxation of the second excited singlet states of aromatic thiones: the role of specific solute-solvent interactions, J. Am. Chem. Soc. 107 (1985) 2831–2837. doi:10.1021/ja00296a001.

[53] D. Bose, D. Sarkar, A. Girigoswami, A. Mahata, D. Ghosh, N. Chattopadhyay, Photophysics and rotational relaxation dynamics of cationic phenazinium dyes in anionic reverse micelles: Effect of methyl substitution, J. Chem. Phys. 131 (2009) 114707. doi:10.1063/1.3225476.

Highlights

- Micellar system induced switching of excimer population of HPFQ
- A competition exists between micellization and polarity to enhance the fluorescence response
- Residence of HPFQ at different regions in differently charged micellar systems
- Electrsostatic interaction and H-bonding play pivotal role in placing HPFQ inside micellar region